AGU PUBLICATIONS

Journal of Geophysical Research: Oceans

Supporting Information for

Secular Trends in Global Tides derived from Satellite Radar Altimetry

I. Bij de Vaate[1], D. C. Slobbe[1], M. Verlaan[2,3]

[1]Civil Engineering and Geosciences, Delft University of Technology, Delft, The Netherlands
[2]Delft Institute of Applied Mathematics, Delft University of Technology, Delft, The Netherlands
[3]Deltares, Delft, Netherlands

Contents of this file

Text S1 and S2.
Figures S1 to S11

Introduction

This supporting information describes the analysis that was performed to assess the sensitivity of estimated S_2 amplitudes to the ionospheric altimetry correction (Text S1) and an assessment of GTSM and UTide-derived confidence intervals using the TPJ-data (Text S2 & Figure S1). In addition, it contains figures (S2-S3) depicting the 95% confidence intervals of the trend estimates based on the confidence intervals of the tidal harmonic constants, as computed by UTide and based on the model approach. Thereafter, Figure S4 and S5 show the co-phase lines derived from satellite altimetry at the start and end of the TPJ-period and the linear changes derived from the SegHA approach (see Section 3.1 in paper) are incorporated in Figure S6 (global) and Figure S7 (North West European Shelf). Finally, Figures S8 to S11 show trends in the tidal amplitude derived from the altimeter corrections for atmospheric propagation and the reference frame offset.

Text S1 Sensitivity Analysis of Estimated Change in S_2 Tidal Harmonic Constants to the Ionospheric Altimeter Correction

One of the geophysical corrections that is applied to the TPJ altimetry data is the ionospheric correction. This can be either an altimeter-derived correction or a modeled correction (NIC09 for TOPEX/Poseidon and GIM for Jason1-3) (Scharroo et al., 2016). As demonstrated by Zawadzki et al. (2018), any error in these corrections would cause a signal at the alias frequency of S_2. In addition, they showed that replacing the altimeter-derived correction with the modeled correction alters the amplitude of the S_2 signal by up to 3 mm.

To assess the sensitivity of the analysis described in the paper to the choice of ionospheric correction, an additional experiment was carried out. For this purpose, the TPJ data of ~500 random crossovers across the globe were corrected by the model-derived ionospheric correction and the radar-derived correction respectively. Consequently, the data were processed and analyzed as described in the paper (following both the SegHA and TintHA approach). The resulting linear change in S_2 amplitudes was compared by computing the median absolute deviation (MAD). Note that crossovers close to land or sea ice were ignored because the radar-derived ionospheric correction is likely deteriorated there (Fernandes et al., 2014).

It was found that the impact of the ionospheric correction was largest near the equator (MAD of up to 0.08 mm/year) and reduced at higher latitudes (< 0.02 mm/year). This is in line with Figure 7 from Zawadzki et al. (2018). The differences were subsequently interpolated to all crossover locations, multiplied by 1.48 to obtain the standard error, and then combined with the standard errors of the S_2 amplitudes that were computed by UTide (Figure S2a) and the model-based alternative (Figure S3a), before multiplying them by the z-score to obtain the final confidence intervals. To get an idea of the impact of the contribution of the ionospheric correction to the uncertainty, one could compare Figures S2a and 6a). As the initial confidence intervals outputted by UTide are the same for all semi-diurnal tides (e.g. S_2 and M_2), the difference between Figure S2a and 6a is solely due to the ionospheric error.

Text S2 Assessment of the Confidence Intervals using Random Subsets of TPJ-data.

To compare the respective performances of the confidence intervals obtained from UTide and those obtained by GTSM, the following experiment was performed. Firstly, the TPJ-data at ~500 random crossovers across the globe were processed. Then, these crossover time series were randomly divided into two time series with half the number of measurements. Subsequently, the linear change in tidal constants was estimated from both time series and the absolute difference was computed. This was done 50 times, resulting in 50 differences for each crossover, tidal constituent, and tidal constant. These differences were then compared to the 95% confidence intervals for the differences, following from error propagation of the 95% confidence intervals for the trend estimates. This was done for respectively the product that was computed by UTide (following from this experiment) and the confidence intervals obtained from GTSM. In the case of the latter, the time series were sampled in a similar way as the TPJ-data in this experiment.

An example of the outcome of this experiment is shown in Figure S1 (for the M_2 amplitude change). As can be seen in Figures S1b and S1c, the confidence intervals obtained by GTSM are at least twice as large as those that followed from UTide. For the M_2 amplitude change, on average 60% of the differences in trend estimates are significant using the UTide confidence intervals, while this is only 6% when the GTSM confidence intervals are applied (see Figures S1d and S1e for global variability). Similar percentages were obtained for S_2: 60% for UTide and 4% for GTSM. For the diurnal tides, the UTide confidence intervals turned out slightly more appropriate (46%), while the GTSM product was consistently accurate (6%).

Concerning the phase change, both confidence intervals perform mediocrely: 54% of the differences are significant following the UTide product, while this is 53% for GTSM (all tides combined). As was also hypothesized in the paper, the fact that the locations of the GTSM reanalysis data are not aligned with the TPJ-data and the location of amphidromic points may affect the quality of the computed confidence intervals, in particular for phase change.

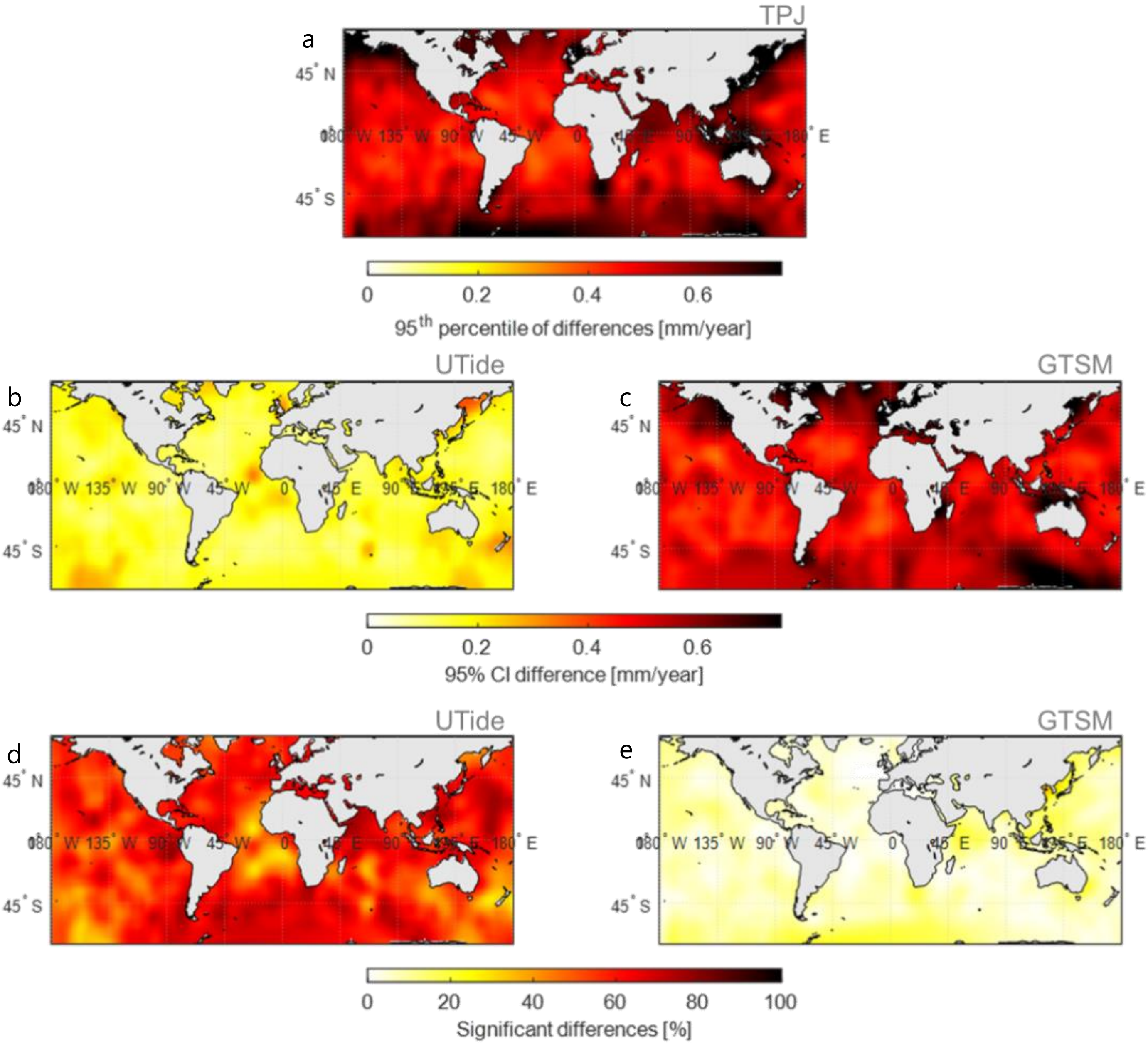

Figure S1. 95th percentile of the differences between M_2 amplitude change estimated from the 50 data division pairs (a). 95% confidence intervals for these differences, as obtained from UTide (b) and GTSM (c). Percentage of the differences that are significant following the UTide (d) and GTSM confidence intervals (e).

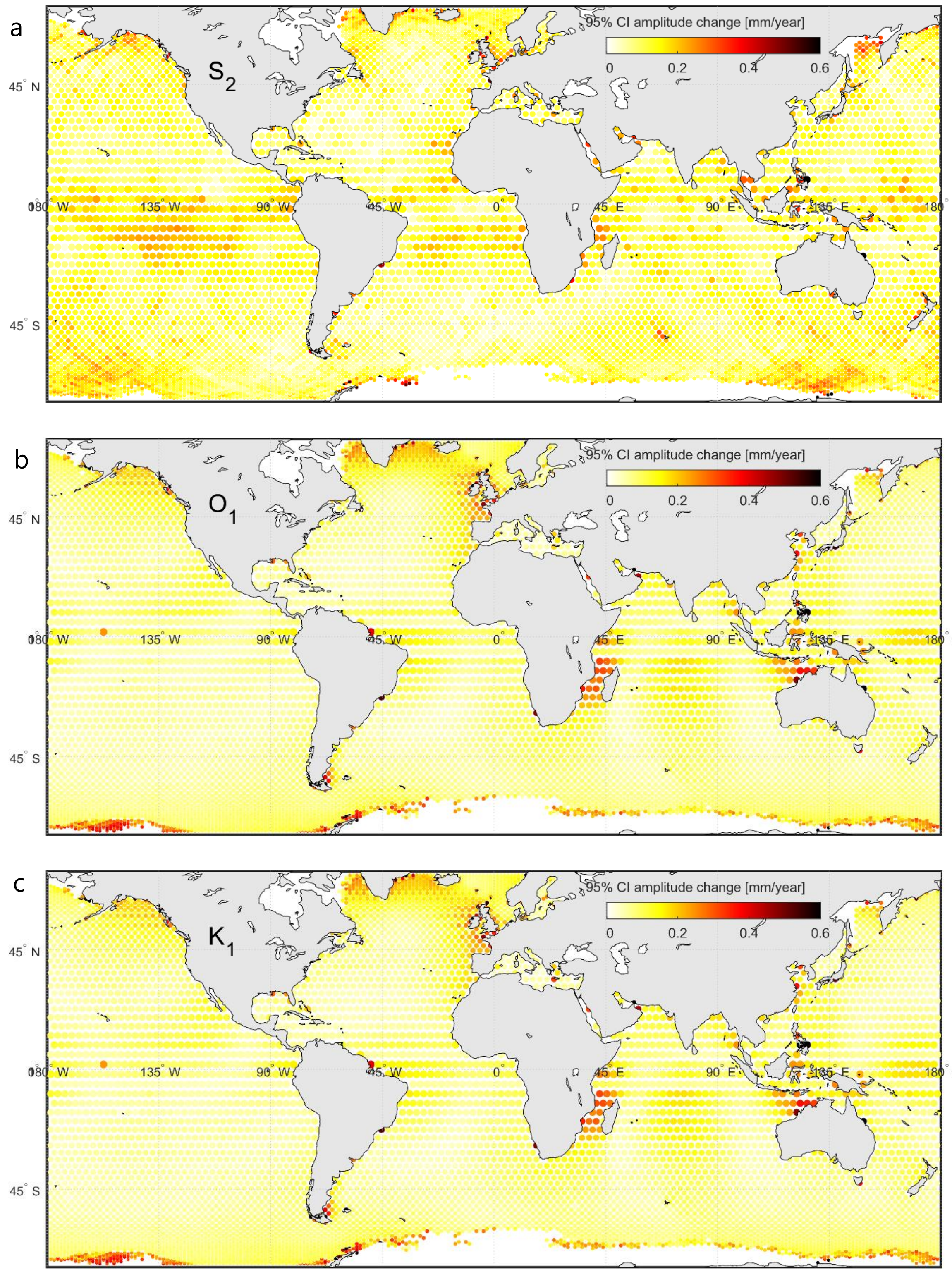

Figure S2. 95% confidence intervals for trend estimates derived from amplitude standard errors computed by UTide following the TintHA approach, for S_2 (a), O_1 (b) and K_1 (c). The intervals for S_2 include the sensitivity to the ionospheric correction as explained in Text S1.

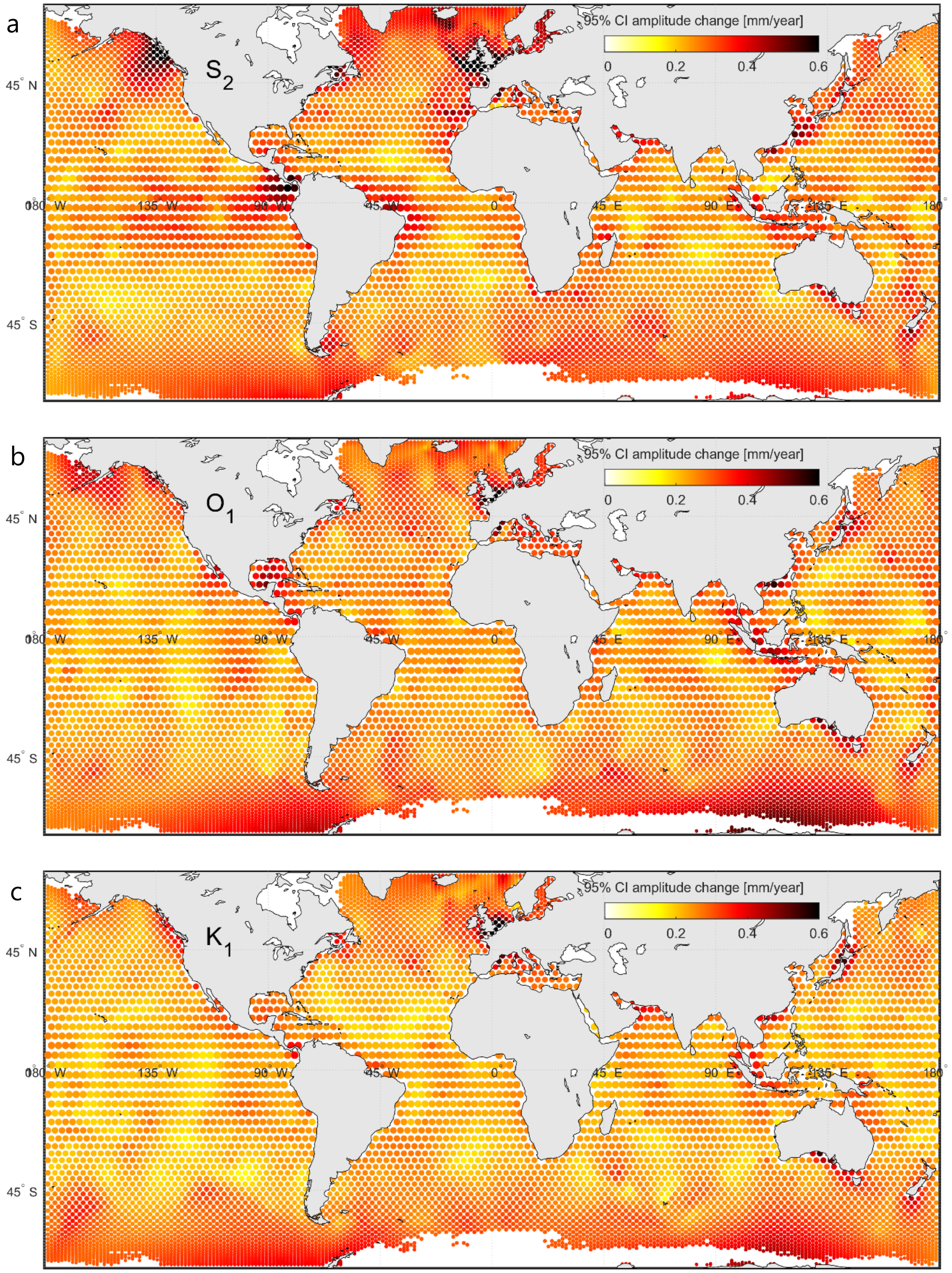

Figure S3. 95% confidence intervals for trend estimates derived from amplitude standard errors derived from model approach described in paper following the TintHA approach, for S_2 (a), O_1 (b) and K_1 (c). The intervals for S_2 include the sensitivity to the ionospheric correction as explained in Text S1.

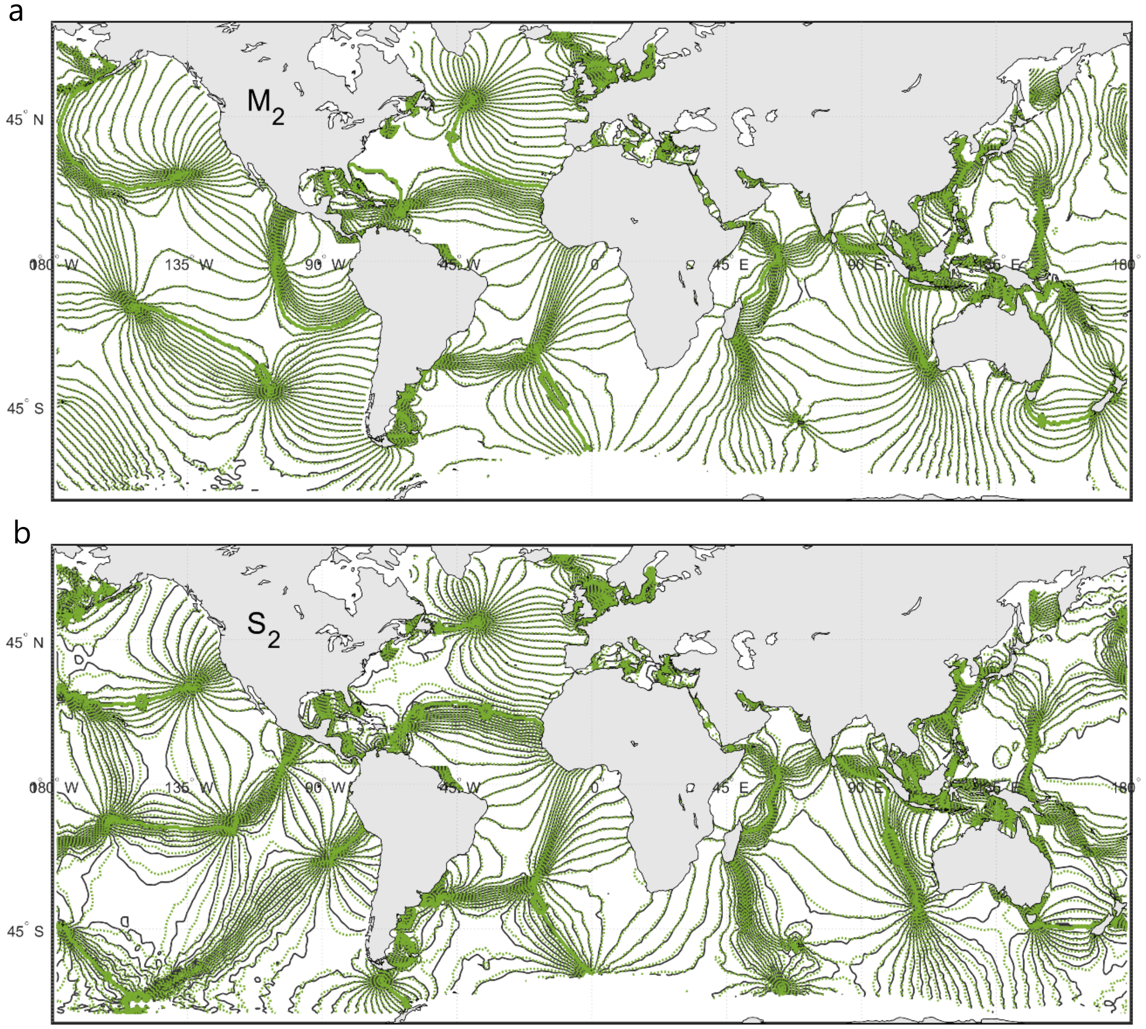

Figure S4. Cotidal phase lines at 10-degree intervals, for 1993 in black and for 2020 in green: M_2 (a), S_2 (b), derived by TintHA approach.

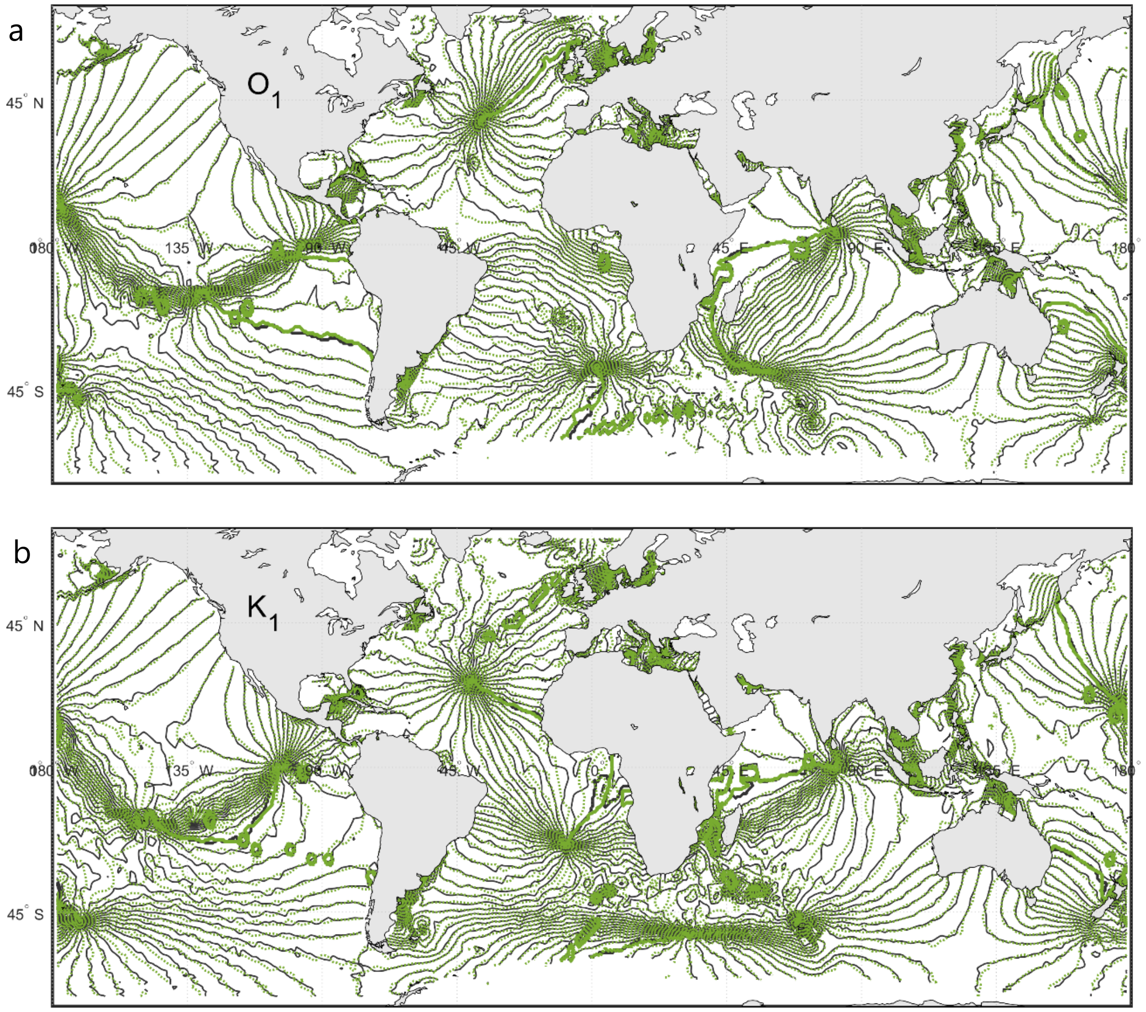

Figure S5. Cotidal phase lines at 10-degree intervals, for 1993 in black and for 2020 in green: O_1 (a), K_1 (b), derived by TintHA approach.

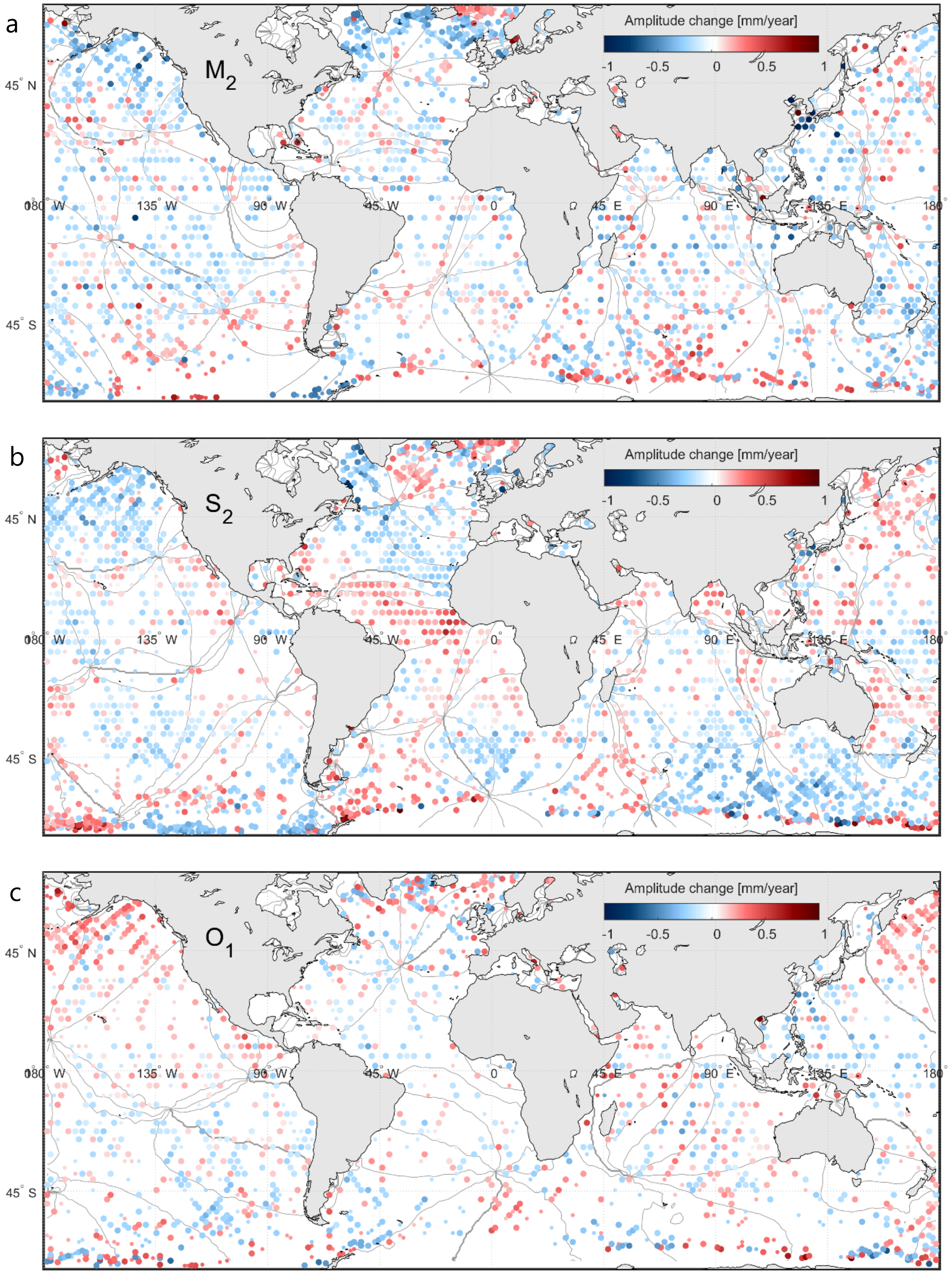

Figure S6. Linear change in M_2 (a), S_2 (b), and O_1 amplitude per year (1993-2020) following the SegHA approach. The smaller scatters indicate data that exceeds both the UTide and GTSM 90% confidence intervals, while the larger scatters indicate significant data at the 95% confidence level. Lines in the background depict tidal phases at 45° intervals.

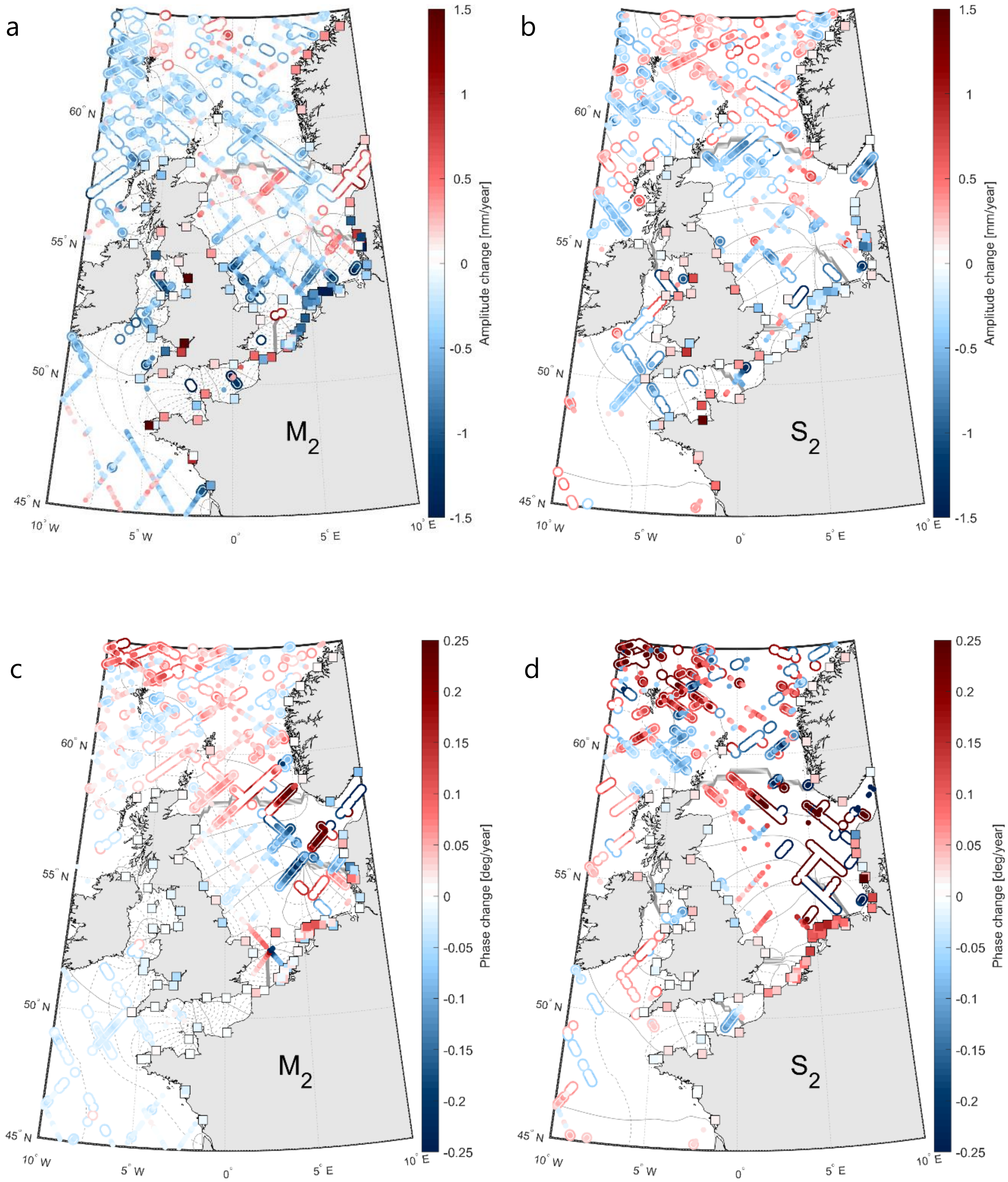

Figure S7. Linear change in M_2 amplitude (a), S_2 amplitude (b), M_2 phase (c) and S_2 phase (d) per year derived by the SegHA approach. The smaller solid scatters indicate significant trends given the UTide 95% confidence intervals, the hollow outline indicates significance according to the GTSM 95% confidence intervals as described in the paper. Co-tidal maps are shown in the background where the solid line indicates the phase at 45° intervals, the dashed lines show the amplitudes at 0.25 m intervals.

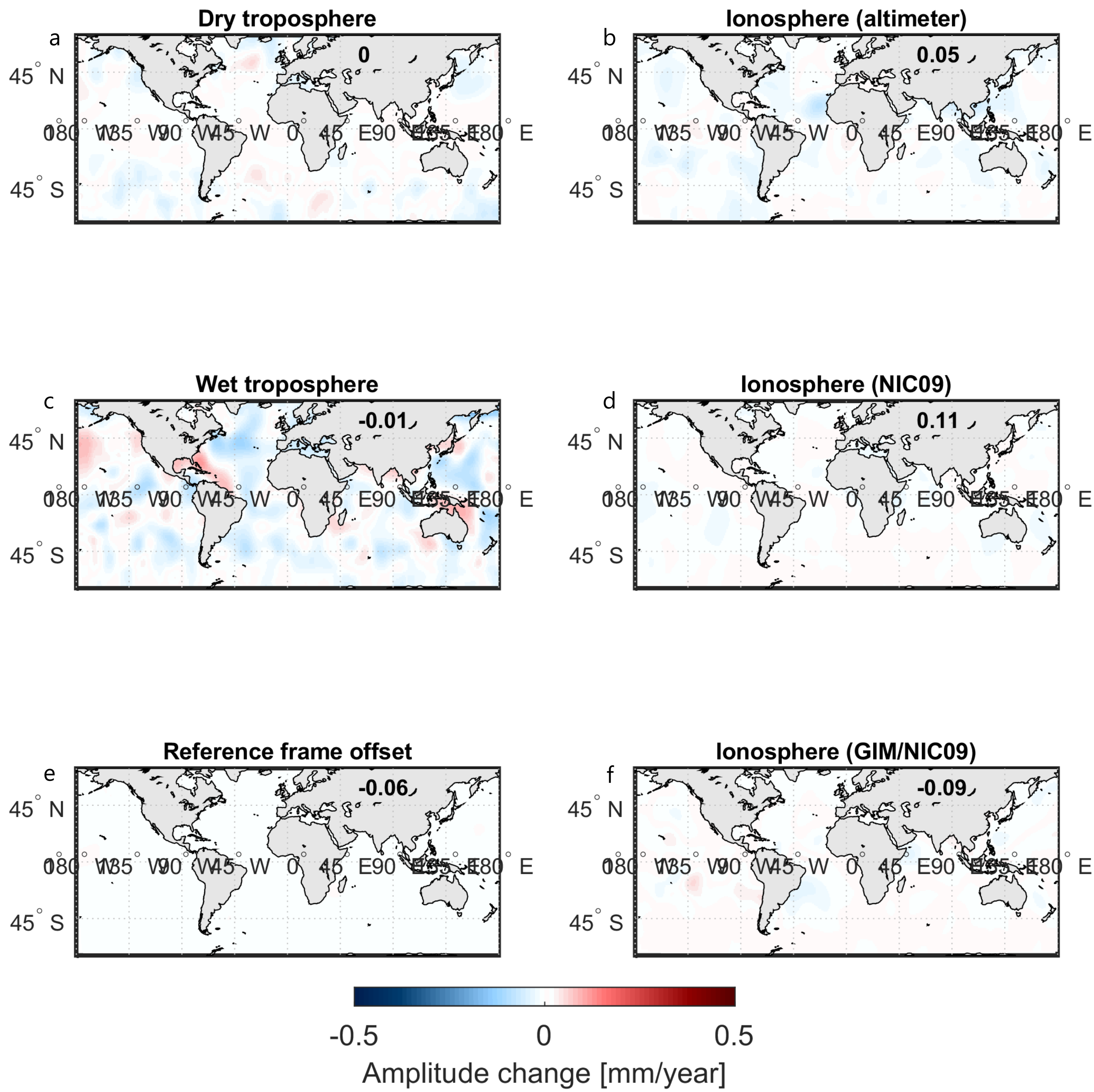

Figure S8. Linear change in M_2 amplitude in the atmospheric propagation corrections (a, b, c, d, f) and reference frame offset correction (e) that were applied to the TPJ data. Data has been interpolated for visualization purposes. The value on top of Russia depicts the correlation coefficient between the change depicted in the figure and the change in M_2 amplitude as presented in the paper (Fig. 2a). Following from the TintHA approach.

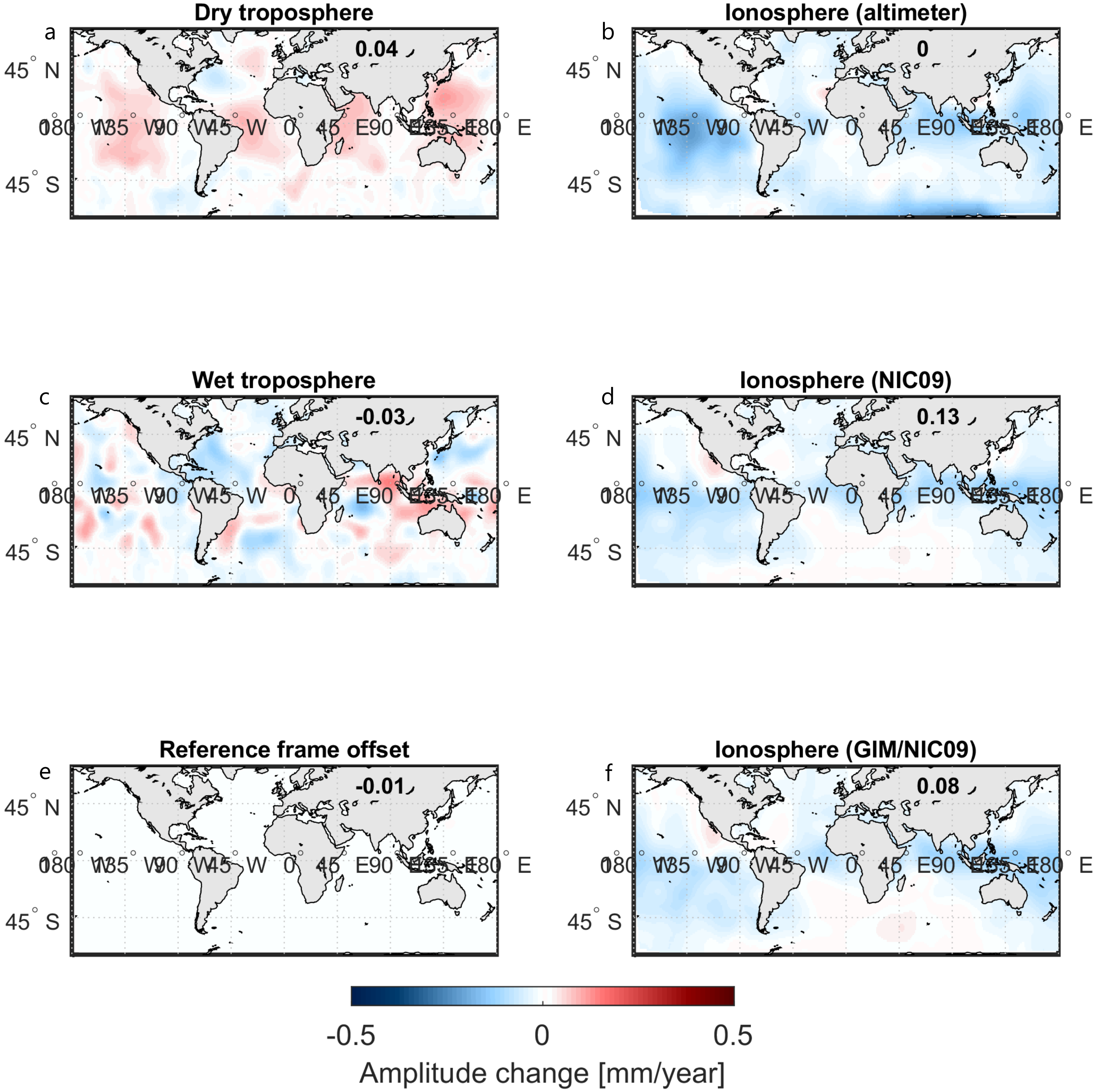

Figure S9. Same as Figure S8 but for S_2.

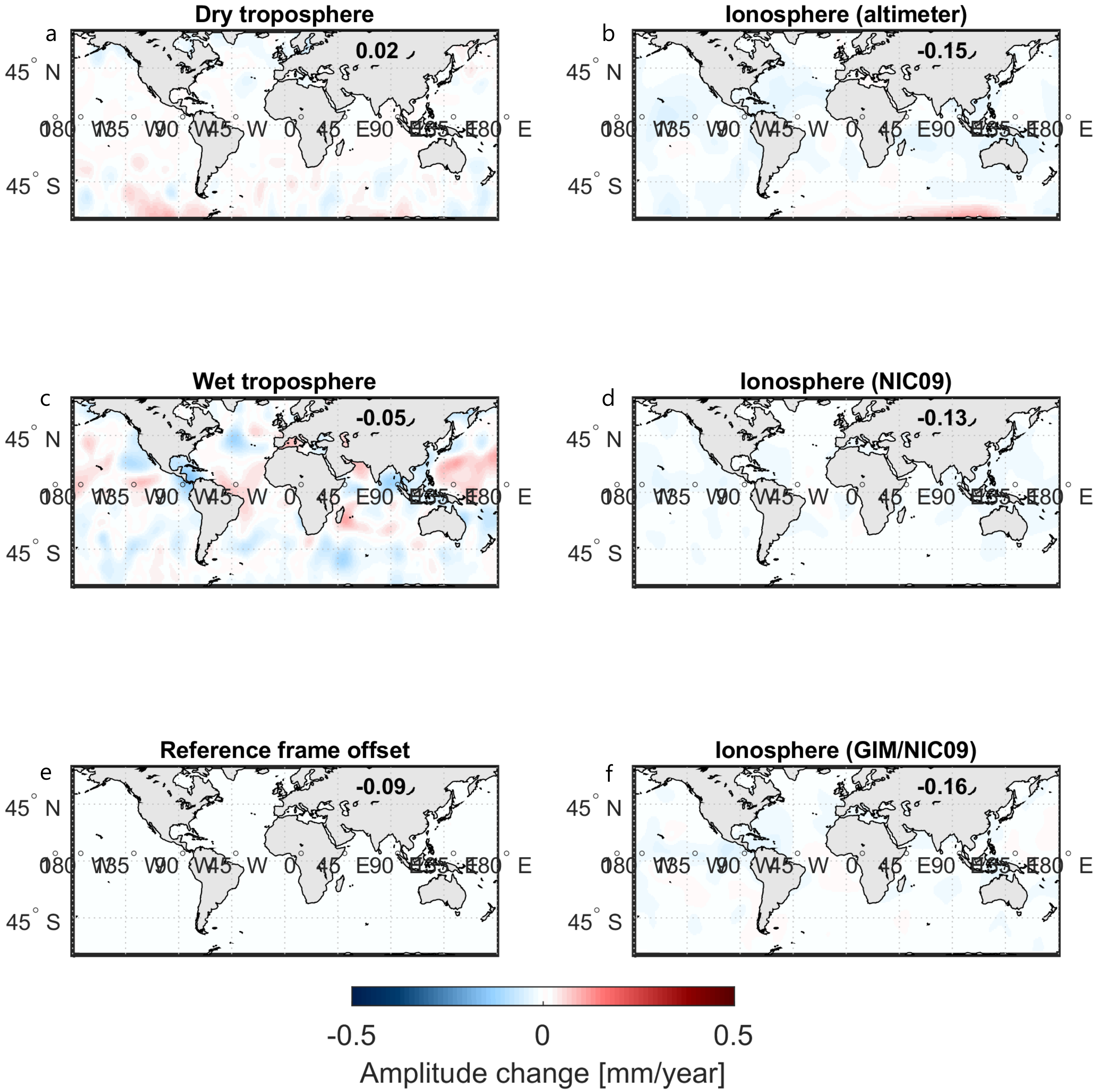

Figure S10. Same as Figure S8 but for O_1.

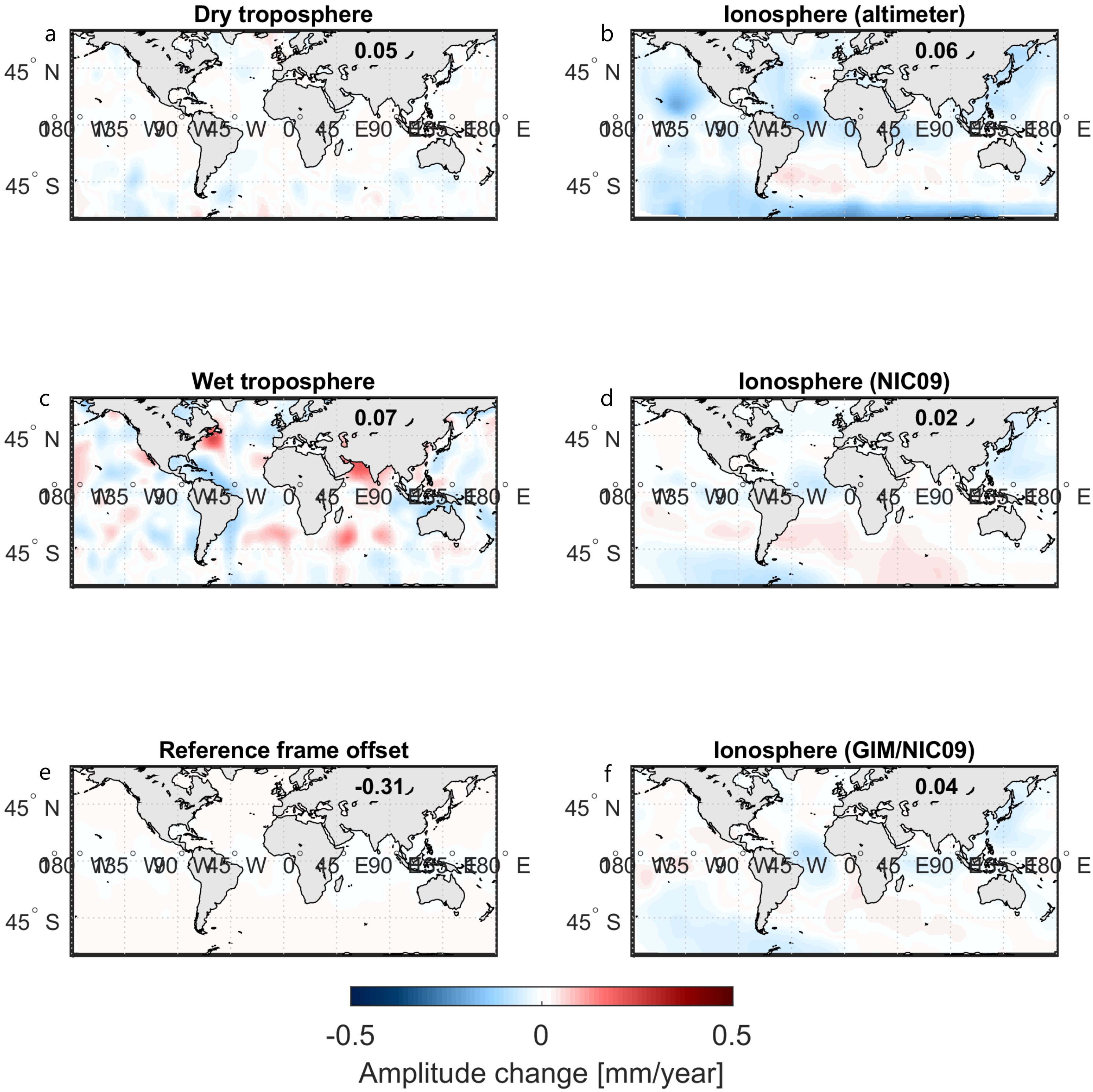

Figure S11. Same as Figure S8 but for K_1.